[Supporting Information]

Selective dual detection of Hg^{2+} and TATP based on amphiphilic conjugated polythiophenes-quantum dot hybrid materials

*Salah M. Tawfik[a], Ali A.Abd-Elaal[a], Yong-Ill Lee[b]**

[a]Department of Petrochemicals, Egyptian Petroleum Research Institute, Cairo 11727, Egypt

[b]Department of Materials Convergence and System Engineering, Changwon National University, Changwon 51140, Republic of Korea

* Corresponding author
E-mail: yilee@changwon.ac.kr (Y-I Lee)
Tel./Fax. (+82) 55-213-3436/213-3439

1. Materials and characterization

The 3-thiopheneacetic acid (98%), *N*,*N*-dimethylethylenediamine (95%), 1-bromooctadecane (97%), 8-hydroxyquinoline, boric acid (99.8%), dicyclohexylcarbodiimide (DCC, 99%), 4-(*N*,*N*-dimethylamino)-pyridine (DMAP, 98%), *N*-hydroxysuccinimide (NHS, 98%), polyethylene glycol (M_n 2000), $CdCl_2$ (99%), Te powder, and $NaBH_4$ were obtained from Sigma-Aldrich and used without further purification. Various metallic salts (AR) including magnesium chloride ($MgCl_2$), stannous chloride ($SnCl_2$), manganese chloride ($MnCl_2$), ferric chloride ($FeCl_3$), cobalt chloride ($CoCl_2$), nickel chloride ($NiCl_2$), copper chloride ($CuCl_2$), zinc chloride ($ZnCl_2$), cadmium nitrate ($Cd(NO_3)_2$), mercury chloride ($HgCl_2$), lead nitrate ($Pb(NO_3)_2$), and chromic chloride ($CrCl_3$) were received from Sigma-Aldrich. The distilled water used in all experiments had a resistivity higher than 18 $M\Omega\cdot cm^{-1}$ from a Milli-Q water purification system.

FT-IR spectra were recorded on an FT/IR-6300 Fourier Transform Infrared Spectrometer (Jasco, Japan). ^{1}H-NMR spectra were recorded at 400 MHz using a Bruker NMR instrument. The fluorescence experiments were performed on an FP-6500 spectrofluorometer (Jasco, Japan) using a quartz cuvette with a 1-cm path length. The absorption spectra were obtained using an Agilent 8543 (Agilent, USA) UV/Vis spectrophotometer. TEM measurements were carried out using a JEM-2100F transmission electron microscope (JEOL, Tokyo, Japan) operating at 200 kV. The XRD powder pattern was obtained on an X'Pert PRO MPD X-ray diffractometer (Analytical, Netherlands) with Cu K_α($K_{\alpha2}$ / $K_{\alpha1}$ =0.5) radiation. DLS analysis was carried out using a Zetasizer Nano ZS90 apparatus (Malvern Instruments, Worcestershire, U.K.).

Safety note

TATP is an extremely dangerous explosive because it shows high sensitivity to friction, temperature changes, and mechanical shocks. Therefore, inexperienced handling of TATP may lead to incapacitating and death. Its synthesis should only be performed in small quantities (about 100 mg) and by highly qualified personnel under the use of appropriate safety measures, such as gloves and reinforced goggles, splinter-proof vessels, and protective shield.[1, 2]

2. Synthesis of monomer 1

Synthesis of N-(2-(dimethylamino)ethyl)-2-(thiophen-3-yl)acetamide

N-(2-dimethylamino)ethyl-2-thiophen-3-yl)acetamide was synthesized according to our previous procedures [3, 4]. Boric acid (0.031 g, 0.5 mmol) was added to a solution of 3-thiophene acetic acid (0.711 g, 5.0 mmol) in toluene (100 mL). *N*,*N*-dimethylethylenediamine (0.443g, 5.0 mmol) was then added in one portion. The reaction mixture was refluxed for 8 h and water was collected azeotropically in the Dean–Stark trap. The mixture was allowed to cool to 40–45 °C, filtered to remove the boric acid present in the reaction mass and further cooled to 25–35 °C. After stirring for 1 h at 25–35 °C, toluene was decanted, and then the resulting crude material was dissolved in methanol (50 mL). Distillation afforded the product (1.01 g, yield 94.92%) as syrup. FT-IR (KBr, Figure 1A), υ= 3280 cm^{-1} (N–H), 3070 cm^{-1} (=C–H), 2910 cm^{-1} (C–H), 1640 cm^{-1} (C=O amide), 1520 cm^{-1} (N-H bond), 1450 cm^{-1} (C=C), 1125 cm^{-1} (C–N). 750 cm^{-1} (C–S). ^{1}H-NMR (D_2O, 400 MHz, Figure 1B): δ= 7.98 (t, 1H, N-H), 7.46 (s 1H, thiophene moiety), 7.22 (d, 1H, thiophene moiety), 7.02 (d, 1H, thiophene moiety), 3.45 (s,2H, -CH_2), 3.19 (m, 2H, -CH_2), 2.28 (m, 2H, -CH_2), 2.106 (s, 6H, -CH_3).

Synthesis of N, N-dimethyl-N-(2-(2-(thiophen-3-yl)acetamido)ethyl)octan-1-aminium bromide

N, N-dimethyl-N-(2-(2-(thiophen-3-yl)acetamido)ethyl)octan-1-aminium bromide was synthesized according to our previous procedures [3, 4]. 1-Bromooctane (0.193 g, 1 mmol) was dissolved in 20 mL of $CH_3OH/(C_2H_5)_2O$ (v/v = 3/2) with the subsequent addition of N-(2-(dimethylamino)ethyl)-2-(thiophen-3-yl)acetamide (0.276 g, 1.3 mmol). The mixture was stirred at room temperature for 12 h. After the reaction was completed, the reaction solution was concentrated to 5 mL. The residue was poured into 200 mL of absolute diethyl ether under stirring and then filtered. The precipitate was filtered, washed with absolute diethyl ether and dried to give yellow waxy compound **monomer 1** (0.44 g, yield 93.89%). FT-IR (KBr, Figure 1A), υ= 3305 cm^{-1} (N–H), 3075 cm^{-1} (=C–H), 2950 cm^{-1} (C–H asy), 2840 cm^{-1} (C–H sy), 2680 cm^{-1} (C–N^+), 1650 cm^{-1} (C=O amide), 1533 cm^{-1} (N-H bond), 1470 cm^{-1} (C=C), 1350 cm^{-1} ($(CH_2)_n$), 1150 cm^{-1} (C–N). 755 cm^{-1} (C–S). ^{1}H-NMR (D_2O, 400 MHz, Figure 1B): δ= 7.95 (t, 1H, N-H), 7.28 (s, 1H, thiophene moiety), 7.15 (d, 1H, thiophene moiety), 6.95 (d, 1H, thiophene moiety), 3.55 (s, 2H, -

CH_2), 3.41 (m, 2H, -CH_2), 3.11 (m, 2H, -CH_2), 2.95 (s, 6H, -CH_3), 2.75-1.11(m, 14H, alkyl chain), 0.88 cm^{-1} (t, 3H, -CH_3).

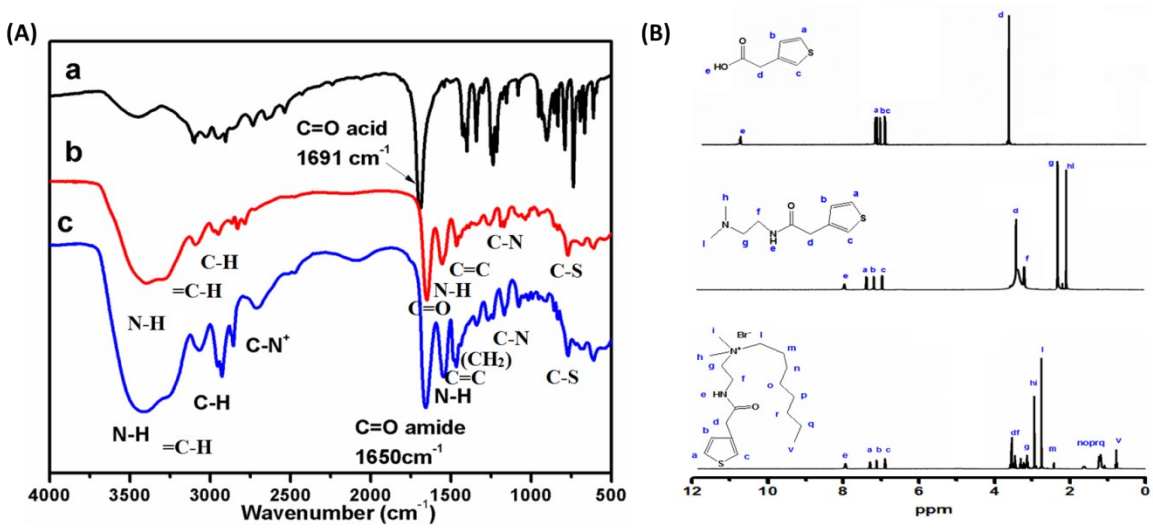

Figure S1. FT-IR (A) ^{1}H-NMR (B) spectra of cationic monomer (a) 3-thiopheneacetic acid, (b) N-(2-(dimethylamino)ethyl)-2-(thiophen-3-yl)acetamide,(c)N,N-dimethyl-N-(2-(2-(thiophen-3-yl)acetamido)ethyl) octan-1- aminium bromide (**monomer 1**).

3. Synthesis of monomer 2

3-thiopheneacetic acid (0.142 g, 1 mmol), PEG-2000 (10 g, 5 mmol), DCC (0.206 g, 1 mmol) and DMAP (0.0244 g, 0.2 mmol) were dissolved in anhydrous DCM (60 mL) and stirred at room temperature for 24 h. The mixture was centrifuged, and the supernatant was concentrated in vacuo (20 mbar, 30 °C), redissolved in DCM (10 mL), and washed with 1 mM HCl (pH 3) (3 × 30 mL), saturated $NaHCO_3$ (3 × 30 mL), and H_2O (3 × 30 mL). The organic phase was dried over $MgSO_4$ for 12 h, filtered, and concentrated in vacuo (20 mbar, 30 °C) to give monomer **2** as a white solid (1.95 g, yield 91.80 %).[3, 4] FT-IR (KBr, Figure S2A), υ= 3470 cm^{-1} (O–H), 3100 cm^{-1} (=C–H), 2900 cm^{-1} (C–H), 1736 cm^{-1} (C=O ester), 1480 cm^{-1} (C=C), 1125 cm^{-1} (C–O), 839 cm^{-1} (C–S). ^{1}H-NMR (D_2O, 400 MHz, Figure 2B): δ= 7.38 (s, 1H, thiophene moiety), 7.23 (d, 1H, thiophene moiety), 7.01 (d, 1H, thiophene moiety), 3.55 (s, 2H, -CH_2), 3.65-4.22 (m, 4H, OCH_2CH_2 in PEG unit), 2.05 (t, 1H, -OH).

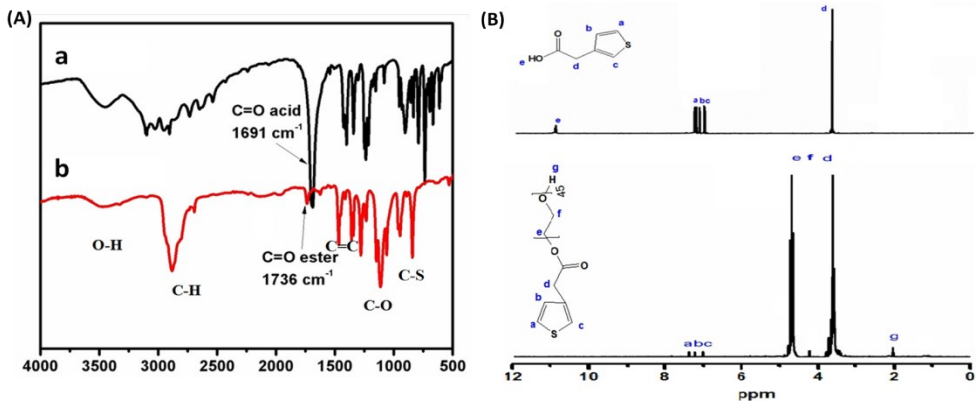

Figure S2. FT-IR (A) ^{1}H-NMR (B) spectra of nonionic monomer (a) 3-thiopheneacetic acid, (b) 3-thiopheneacetic acid-PEG2000 **(monomer 3)**.

4. Synthesis of monomer 3

Synthesis of quinolin-8-yl 2-(thiophen-3-yl)acetate

Quinolin-8-yl 2-(thiophen-3-yl)acetate was prepared according to our previous procedures.[3, 4] 3-thiopheneacetic acid (1.42 g, 10 mmol), 8-Hydroxyquinoline (1.45 g, 10 mmol), DCC (2.06 g, 10 mmol) and DMAP (0.488 g, 4 mmol) were dissolved in anhydrous DCM (40 mL) and stirred at room temperature for 24 h. The mixture was centrifuged and the supernatant was concentrated in vacuo (20 mbar, 30 °C) redissolved in DCM (10 mL), and washed with 1 mM HCl (pH 3) (3 × 30 mL) saturated $NaHCO_3$ (3 × 30 mL), and H_2O (3 × 30 mL). The organic phase was dried over $MgSO_4$ for 12 h, filtered, and concentrated in vacuo (20 mbar, 30 °C) to give quinolin-8-yl 2-(thiophen-3-yl) acetate as a brown solid (2.32 g, yield 86.24 %). FT-IR (KBr, Figure 3A), υ= 3090 cm^{-1} (=C–H), 2955 cm^{-1} (C–H), 1748 cm^{-1} (C=O ester), 1610 cm^{-1} (C=C benzene), 1120 cm^{-1} (C–N), 782 cm^{-1} (C–S). ^{1}H-NMR (D_2O, 400MHz, Figure 3B): δ= 7.66-8.93 (m, 6H, quinoline moiety), 7.51 (s, 1H, thiophene moiety), 7.45 (d, 1H, thiophene moiety), 7.20 (d, 1H, thiophene moiety), 3.50 (s, 2H, $-CH_2$).

Synthesis of 1-octyl-8-(2-(thiophen-3-yl)acetoxy)quinolin-1-ium bromide (monomer 4)

1-octyl-8-(2-(thiophen-3-yl)acetoxy)quinolin-1-ium bromide was prepared according to our previous procedures.[3, 4] 1-Bromooctane (0.193 g, 1 mmol) was dissolved in 20 mL of CH_2Cl_2/CH_3OH (v/v = 3/2) with the subsequent addition of quinolin-8-yl 2-(thiophen-3-yl)acetate (0.276 g, 1.3 mmol). The mixture was stirred at room temperature for 24 h. After the reaction was

completed, the reaction solution was concentrated to 5 mL. The residue was poured into 200 mL of absolute diethyl ether under stirring and then filtered. The precipitate was washed with absolute diethyl ether and dried to give compound **monomer 3** (0.39 g, yield 83.15%) as a yellow powder. FT-IR (KBr, Figure S3A), υ= 3050 cm^{-1} (=C–H), 2960 cm^{-1} (C–H_{asy}), 2875 cm^{-1} (C–H sy), 1750 cm^{-1} (C=O ester), 1590 cm^{-1} (C=C benzene), 1360 cm^{-1} ($(CH_2)_n$), 1100 cm^{-1} (C–N), 794 cm^{-1} (C–S). ^{1}H-NMR (D_2O, 400 MHz, Figure 3B): δ= 7.98-8.96 (m, 6H, quinoline moiety), 7.81 (s, 1H, thiophene moiety), 7.35 (d, 1H, thiophene moiety), 7.31 (d, 1H, thiophene moiety), 3.45 (s, 2H, -CH_2), 3.21-2.11(m, 14H, alkyl chain), 1.02 cm^{-1} (t, 3H, -CH_3).

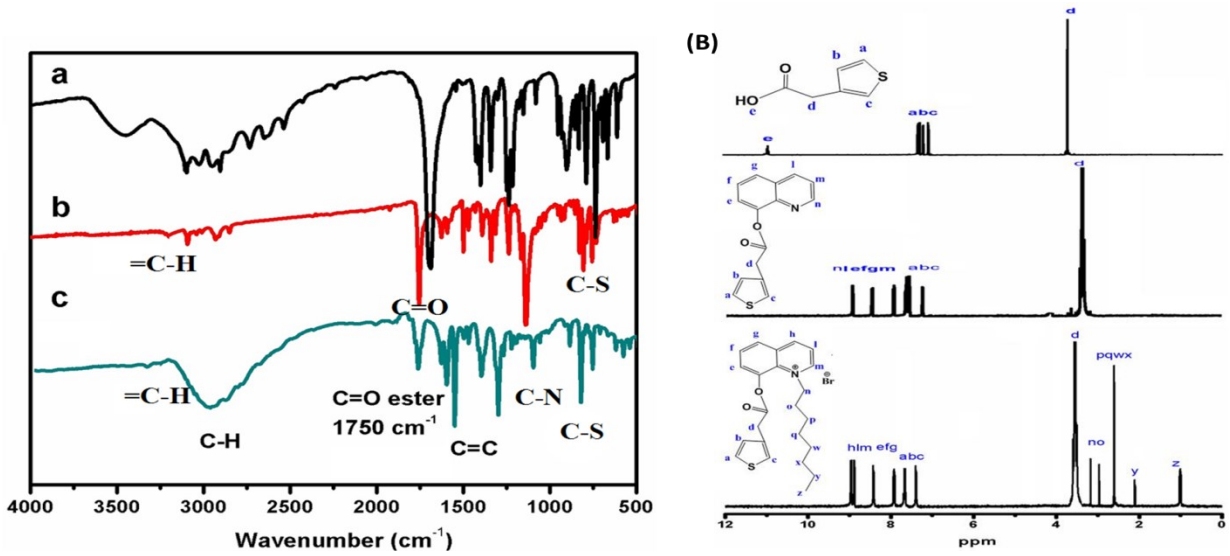

Figure S3. FT-IR (A) ^{1}H-NMR (B) spectra of conjugated cationic monomer (a) 3-thiopheneacetic acid, (b) quinolin-8-yl 2-(thiophen-3-yl)acetate, (c) 1-octyl-8-(2-(thiophen-3-yl)acetoxy) quinolin-1-ium bromide (**monomer 3**).

5. Synthesis of CdTe QDs coated thiophene copolymer via in situ polymerization in aqueous solution (PQDs)

PQDs was synthesized according to our previously reported procedures [3, 4]. Briefly, under N_2 atmosphere 15 mL aqueous solution of the three prepared monomers, M1 (0.03 mmol), M2 (0.04 mmol) and M3 (0.004 mmol)) were added to 5 mL of CdTe QDs (pH 7) followed by stirring for 30 min, then 0.6 mmol of $(NH_4)_2S_2O_8$ was added by drop-wise into the mixture. The mixture was stirred for 24 h at 25 ± 1 °C, then 20 ml of methanol was added to precipitate the PQDs nanoparticle. The prepared nanomaterials were collected by filtration and washed with acetone via stirring for 3 h to remove residual oligomers and initiator. The prepared nanoparticles were air-dried overnight, followed by drying under vacuum (Scheme 1).

PQDs: FT-IR (KBr, Fig 1a), υ= 3500 cm^{-1} (O–H), 3350 cm^{-1} (N–H), 3090 cm^{-1} (=C–H), 2980 cm^{-1} (C–H asy), 2887 cm^{-1} (C–H sy), 1745 cm^{-1} (C=O ester), 1650 cm^{-1} (C=O amide), 1500 cm^{-1} (N-H bond), 1200 cm^{-1} (C–O), 1050 (C–N), 767 cm^{-1} (C–S). ^{1}H-NMR (D_2O, 400 MHz, Fig S4): δ= 7.33-9.12 (m, 6H, quinoline moiety), 8.33 (t, 1H, N-H), 7.11 (s, 1H, thiophene moiety), 6.95 (s, 1H, thiophene moiety), 6.77 (s, 1H, thiophene moiety), 4.31 (s, 2H, $-CH_2$), 3.55-4.66 (m, nH, OCH_2CH_2 in PEG unit), 2.56 (s, 6H, $-CH_3$), 2.11 (t, 1H, -OH), 1.36-0.91(m, nH, alkyl chain), 0.91 cm^{-1} (t, 3H, $-CH_3$).

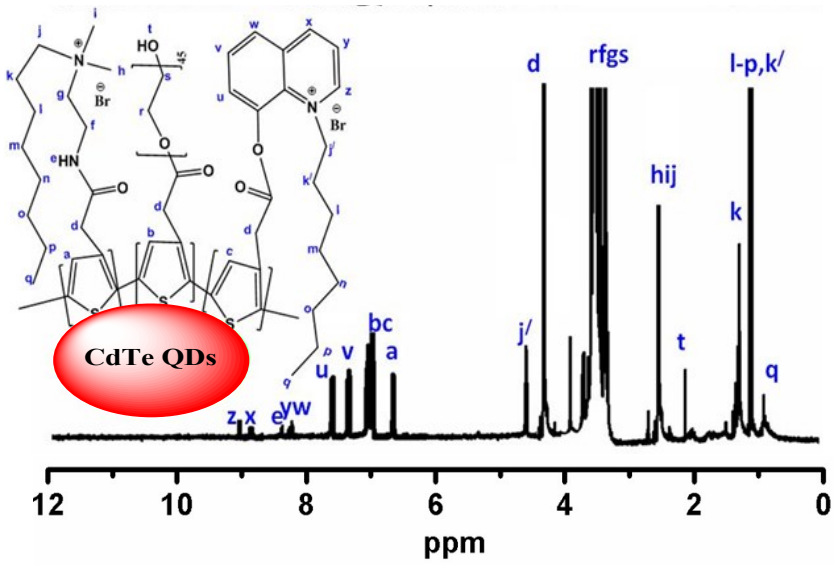

Fig. S4. ^{1}H-NMR spectra of CdTe QDs coated with thiophene copolymer (PQDs).

170 **6. The determination of photoluminescence quantum yield (PLQY)**

171 The quantum yields of CdTe QDs and PQDs were determined by comparing the integrated FL
172 intensities and the absorbance values of the QDs with the reference, rhodamine B (Φ = 0.31), and
173 the as-prepared QDs were dissolved in water (n = 1.33). A UV−vis absorption spectrometer was
174 used to determine the absorbance values of the samples at 350 and 380 nm excitation wavelengths,
175 respectively. The spectrophotometer set with an excitation slit width of 3 nm and an emission slit
176 width of 3 nm was used to excite the samples to record their FL spectra. The PLQY was calculated
177 using the equation (1) below [5].

178
$$\Phi_x = \Phi_r \times \frac{I_x}{I_r} \times \frac{A_x}{A_r} \times \frac{n_x^2}{n_r^2} \quad (1)$$

179 where Φ_x is the PLQY, I is the integrated fluorescence intensity, A is the absorbance, and n is the
180 refractive index of the solvent; *r* denotes the standard and *x* denotes the sample.

181 **7. Biocompatibility**

182 To assess the biocompatibility of the PQDs in comparison with the pristine CdTe QDs, an MTT
183 cell assay was performed on the HeLa cells. Briefly, HeLa cells were plated at a density of 1×10^4
184 cells per well in a 96-well plate, and then incubated for 24 h at 37 °C under 5% CO_2 to allow the
185 cells to attach to the wells. The PQDs and CdTe QDs were sterilized by autoclaving, and then
186 serial dilutions of the QDs at a different concentrations of 400 and 600 $\mu g \cdot mL^{-1}$ were added to the
187 culture wells to replace the original culture medium and were incubated for another 24 h in 5%
188 CO_2 at 37 °C. Next, 100 mL of MTT solution (dissolved in RPMI 1640) was added to each well
189 (containing different amounts of the PQDs and pristine CdTe QDs, followed by incubation for 4
190 h inside a CO_2 incubator at 37 °C. After incubation, the medium was removed, and the formed
191 formazan crystals were dissolved in 100 μL of DMSO/ethanol mixture (1:1). A Tecan Infinite
192 M200 monochromator-based multifunction microplate reader was used to measure the OD 570
193 (Abs value) of each well with background subtraction at 540 nm. At least three independent
194 experiments were performed in each case. The following equation (2) was applied to calculate the
195 viability of cell growth [6] :

196 $$Cell\ viability\ (\%) = \frac{mean\ Abs\ value\ of\ treatment\ group}{mean\ Abs\ value\ of\ control} \times 100 \qquad (2)$$

197 Table S1. Comparison of developed fluorescence method with some similar methods reported in
198 literature for the determination of Hg^{2+}.

Detection method	Linear range (μM)	LOD (nM)	Ref.
CDs	0-80	201	7
Au/N-CQDs	0-41.86	118	8
Fluorescence polymer	0.2-2	370	9
Rhodamine labeled cellulose nanocrystals	0-100	232	10
Ferrocenyl-naphthalimide	-------	794	11
Rhodanine-stabilized gold nanobipyramids	0.6-50	200	12
Zr-based MOFs	0-13	500	13
solothiocarbonyl quinacridone	0-60	140	14
COF-LUZ8	0.5-5	125	15
AH-COF	0-100	100	16
Hollow MnFeO oxide	0.1-15	20	17
Tetraphenylethene derivatives	0-100	20	18
Near-infrared ratiometric fluorescent carbon dot-based nanohybrid	0-40	9	19
Conjugated polythiophenes-coated CdTe QDs	0.5-64	7.4	This work

199

200

201 Table S2. Comparison of developed fluorescence method with some similar methods reported in
202 literature for the determination of TATP.

Detection method	Step 1: process for TATP hydrolysis to H_2O_2 (needed time)	Step 2: process for H_2O_2 detection (needed time)	Real Sample	Linear range (mg L^{-1})	LOD (mg L^{-1})	Ref.
Colorimetric	Acidic degradation (5 min)	Fe_3O_4 MNPs catalyzed colorimetric reaction (30 min)	Synthetic complex, and contaminated soil samples	1-10	0.47	[20]
Colorimetric	Hydrolysis by acidic cation exchanger resin (30 min)	AgNPs-based colorimetric reaction (30 min)	Synthetic complex samples	1.25-31.25	0.31	[21]
CL	Acidic degradation-flow system (2 min)	Cu^{2+}- catalyzed CL system (1 min)	Synthetic samples	0.22-44	0.11	[22]
CL	Acidic degradation (5 min)	HRP- catalyzed CL system (1 min)	Contaminated materials and to spiked soils	0.1-13.3	0.04	[23]
Fluorescence	solid acid catalysis, i.e., amberlyst-15	turn-on fluorescence responses (5 sec)	-------	-------	0.1	[24]
Colorimetric	Acidic degradation of TATP (5 min)	Ag@ZnMOF catalyzed colorimetric system (6 min)	Apple juices and water samples	0.4-15	0.1	[25]
Fluorescence	----------	30 min	--------	0.5-8	0.5	[26]
Colorimetric	acidic hydrolysis	degradation of TATP in the presence of MnO_2 nanozymes	Detergent	1.57 -10.50	0.34	[27]
Fluorescence-PQDs-Hg^{2+}	----------	----------	river water	2.5-50	0.055	this work

203 LOD: limit of detection, MNPs: Magnetic Nanoparticles, AgNPs: silver nanoparticles, CL: chemiluminescence, HRP:
204 horseradish peroxidase, Ag@ZnMOF: silver nanoparticle/flake like zinc metal organic framework.

205

206

207

References

1. M. E. Germain and M. J. Knapp, *Inorganic Chemistry*, 2008, **47**, 9748-9750.
2. Y. Qi, W. Xu, N. Ding, X. Chang, C. Shang, H. Peng, T. Liu and Y. Fang, *Materials Chemistry Frontiers*, 2019, **3**, 1218-1224.
3. S. M. Tawfik, M. Sharipov, S. Kakhkhorov, M. R. Elmasry and Y.-I. Lee, *Advanced Science*, 2019, **6**, 1801467.
4. S. M. Tawfik, J. Shim, D. Biechele-Speziale, M. Sharipov and Y.-I. Lee, *Sensors and Actuators B: Chemical*, 2018, **257**, 734-744.
5. J. Xue, X. Chen, S. Liu, F. Zheng, L. He, L. Li and J.-J. Zhu, *ACS Applied Materials & Interfaces*, 2015, **7**, 19126-19133.
6. X. Peng, Q. Long, H. Li, Y. Zhang and S. Yao, *Sensors and Actuators B: Chemical*, 2015, **213**, 131-138.
7. J. He, H. Zhang, J. Zou, Y. Liu, J. Zhuang, Y. Xiao, B. J. B. Lei and Bioelectronics, 2016, **79**, 531-535.
8. A. Meng, Q. Xu, K. Zhao, Z. Li, J. Liang, Q. J. S. Li and A. B. Chemical, 2018, **255**, 657-665.
9. U. Haldar and H.-i. Lee, *ACS Applied Materials & Interfaces*, 2019, **11**, 13685-13693.
10. X. Ye, Y. Kang and J. J. C. Zhou, 2020, **27**, 5197-5210.
11. J. Dong, J. Hu, H. Baigude and H. J. D. T. Zhang, 2018, **47**, 314-322.
12. Y. Qi, J. Zhao, G.-j. Weng, J.-j. Li, X. Li, J. Zhu and J.-w. J. J. o. M. C. C. Zhao, 2018, **6**, 12283-12293.
13. Z. Wang, J. Yang, Y. Li, Q. Zhuang and J. J. D. T. Gu, 2018, **47**, 5570-5574.
14. Y. Qu, Y. Jin, Y. Cheng, L. Wang, J. Cao and J. J. J. o. M. C. A. Yang, 2017, **5**, 14537-14541.
15. S.-Y. Ding, M. Dong, Y.-W. Wang, Y.-T. Chen, H.-Z. Wang, C.-Y. Su and W. J. J. o. t. A. C. S. Wang, 2016, **138**, 3031-3037.
16. Y. Yu, G. Li, J. Liu and D. J. C. E. J. Yuan, 2020, **401**, 126139.
17. Z. Lu, Y. Dang, C. Dai, Y. Zhang, P. Zou, H. Du, Y. Zhang, M. Sun, H. Rao and Y. Wang, *Journal of Hazardous Materials*, 2021, **403**, 123979.
18. L. Zhao, Z. Zhang, Y. Liu, J. Wei, Q. Liu, P. Ran and X. Li, *Journal of Hazardous Materials*, 2020, **385**, 121556.
19. J. Zhao, M. Huang, L. Zhang, M. Zou, D. Chen, Y. Huang and S. Zhao, *Analytical Chemistry*, 2017, **89**, 8044-8049.
20. Z. Can, A. Üzer, K. Türkekul, E. Erçağ and R. Apak, *Analytical Chemistry*, 2015, **87**, 9589-9594.
21. A. Üzer, S. Durmazel, E. Erçağ and R. Apak, *Sensors and Actuators B: Chemical*, 2017, **247**, 98-107.
22. P. Mahbub, P. Zakaria, R. Guijt, M. Macka, G. Dicinoski, M. Breadmore and P. N. Nesterenko, *Talanta*, 2015, **143**, 191-197.
23. S. Girotti, E. Ferri, E. Maiolini, L. Bolelli, M. D'Elia, D. Coppe and F. S. Romolo, *Analytical and Bioanalytical Chemistry*, 2011, **400**, 313-320.
24. X. Yu, Y. Gong, W. Xiong, M. Li, J. Zhao and Y. Che, *Analytical Chemistry*, 2019, **91**, 6967-6970.
25. N. Bagheri, A. Khataee, J. Hassanzadeh and B. Habibi, *Journal of Hazardous Materials*, 2018, **360**, 233-242.
26. Y. An, X. Xu, K. Liu, X. An, C. Shang, G. Wang, T. Liu, H. Li, H. Peng and Y. J. C. C. Fang, 2019, **55**, 941-944.
27. S. R. Hormozi Jangi, M. Akhond and G. Absalan, *Microchimica Acta*, 2020, **187**, 431.